CANADA
DEPARTMENT OF ENERGY, MINES AND RESOURCES
Observatories Branch

PUBLICATIONS
of the
DOMINION OBSERVATORY
OTTAWA

Volume XXXIX • No. 2

A SYSTEM OF MAGNETIC ANALYSIS FOR IONOSPHERIC CURRENTS

Ralph D. Hutchison

THE QUEEN'S PRINTER
OTTAWA, 1970

Contents

A SYSTEM OF MAGNETIC ANALYSIS FOR IONOSPHERIC CURRENTS

Ralph D. Hutchison*

ABSTRACT: The magnetic field of a circular-line current can be expressed (in complete elliptic integrals) so that there are no regions of mathematical failure or weakness. Such an expression is set up in spherical co-ordinates suitable to the study of ionospheric currents. It is shown that magnetic observations on the surface of the earth can then be used analytically to define current strength, height of current path, and curvature of current path. The analytical system is capable of development for coping with ribbon currents or more elaborate cases, though the present work does not extend beyond a selection of simple-line currents.

RÉSUMÉ: Le champ magnétique d'un courant linéaire circulaire peut être exprimé (en intégrales elliptiques complètes) de façon à ce qu'il n'y ait pas de zones de défaillance ou de faiblesse mathématique. Cette expression est représentée en coordonnées sphériques appropriées à l'étude des courants ionosphériques. L'auteur démontre que les observations magnétiques effectuées à la surface de la terre peuvent alors être utilisées analytiquement pour définir la force du courant ainsi que la hauteur et la courbure de sa trajectoire. Le système analytique peut être élaboré de façon à tenir compte des courants rubanés, ou de cas plus complexes, bien que l'étude actuelle se limite au choix de courants linéaires simples.

Introduction

This paper arises from a research problem posed by Dr. P.H. Serson, chief of the Division of Geomagnetism, Dominion Observatory, Ottawa. The requirement is for an analytical system by which ionospheric current patterns can be deduced from magnetic observations on the ground.

Dr. Serson's outline of the case refers to plans for special observations of auroral displays and their associated electrical currents – auroral electrojets – during the coming maximum of solar activity. Rocket flights, for a variety of measurements within auroral displays, are one part of the general plan. Another part is to establish a grid of recording magnetometers on the ground; these would provide independent information, of a different sort from that obtainable in rocket flights.

Arrangements were made in September 1967 for a pilot research project, to investigate the analytical problem. Some success can now be reported. A mathematical description is developed for an elementary physical case that represents an ionospheric current under the usual conditions for ground observation. Analytically useful functions are drawn from it; and they are capable of extension for dealing with more complex cases.

Statement of Case

For the ionospheric problem a suitable concept, or mathematical model, is that of a circular line current and its associated magnetic field. The current path is a circle of any radius lying in a particular spherical surface – the ionosphere. Observations on the earth imply a second spherical surface, slightly smaller than the first.

An exact mathematical description of the case forms a basis for the development of analytical techniques. Significant elementary functions are found. The compounding of elementary functions to describe a more elaborate current system is a further step – beyond the scope of the present work, but partly covered in earlier published work.

The above is strictly synthesis. Analysis is the converse. A given set of observations may show only one set of elementary functions, of the proper sort to define a simple line current. If it shows more, it can be resolved into components, perhaps several sets of elementary functions, each of which is a valid description of some part of the total physical case. Thus information is derived.

It may be noted that this principle is not the same as harmonic analysis. Periodic functions (sines, cosines, Legendre functions) are a type of element much used, and having specific powers for world-wide problems. A physical case can be approximately described by a sufficient number of such elements in an ordered series (Fourier's principle); the series as a whole then has physical significance, though its elements describe nothing real.

A geophysical anomaly can often be called a wave form, an isolated wave, not part of a wave train. To represent it by a sum of periodic waves may be a clumsy method of approximation. Geophysical studies lead to elementary functions which are, in effect, single waves, each appropriate to an elementary physical case.

The anomaly of the ionospheric current loop is the magnetic disturbance observable on the ground (or elsewhere). Most of the disturbance is in the near vicinity of the current path, and in cross section it has a wave form appropriate to the current distribution. With increasing distance from the current path, the anomaly fades out as a transient. Hence a local set of observations may define only part of a current loop, not the whole of it if the loop is large.

It is found in the present study that such observations can define current strength, height of current path, and curvature of current path. It should also be possible to distinguish separate current systems if each is roughly a line concentration and if there is reasonable distance between them; reasonable

*Consulting Geophysicist, 92 Glenview Ave., Toronto 12, Ontario.

distance would be something like 100 km or more – the height of the ionosphere in round figures. This sort of distinction would serve to identify induced currents, whether near surface or at depth in the earth.

Principal Conclusions

Some of the following items deal with the collecting and analyzing of field data. They are not all specific conclusions from the present study, nor are they all discussed in other parts of the report. Some represent general rules of geophysics or of survey practice.

1. The chief aim is to find and define ionospheric current systems from ground magnetic records. The auroral zone is well enough known that a traverse, or line of recording stations, can be positioned where it will bracket a reasonable number of the probable auroral electrojets. A single traverse directed geomagnetic north would be highly effective for analytical data. There are permanent stations for coarse mapping of field patterns. Churchill is mentioned as a base for rocket experiments and other things; there might be arguments for siting the main magnetic traverse farther west, to avoid coupling effects from Hudson Bay; nevertheless, such coupling is information that should not be totally avoided.

2. A station interval of 100 km would be generally adequate, but a considerably smaller interval – say about 20 km – could be useful in looking for detail. For example, a small loop current related to an electrojet might remain stable long enough to drift across the fixed traverse and thus be more or less fully mapped. But its characterictic profile is something like that of an antiparallel pair of line currents, and with only coarse mapping the two might be confused. The small-loop anomalies illustrated in Figures 3, 4 and 7 of this report are clearly not going to be well defined by observations 100 km apart; 50 km would serve, a smaller interval would be better. The same sort of argument would apply to the analytical distinction between a line current and a ribbon current; the elementary functions for the two cases are the same in coarse characteristics but they differ in detail. And again, the same sort of argument might apply in the distinction between a primary ionospheric current and any induced earth currents. There is also a 'noise' argument for avoiding a theoretical minimum of stations: certain stations may be less than fully effective because of purely local disturbance factors that distort the field under observation.

3. The previous point is hardly clear enough for planning a specific survey grid. Further contributions should come from someone well acquainted with electrojet habits. A compound traverse might be well worth considering, the whole to cover a length equivalent to ten or more degrees of latitude, with a close station interval over part of it – say 20 miles, rather than 20 km, between stations – and a coarser interval over the rest. This can be considered a sort of hunting or ambush layout: interesting details might appear from time to time in the section prepared for them; information in less detail would register in other sections. Part of the detail section might be expanded from a simple traverse to a square grid, for a more decisive mapping of small loops, or equivalent anomalies, that might pass that way. Neither a straight traverse nor a uniform station interval is really required, unless for some computer process.

4. The correlation and analysis of geophysical data is often a bigger job than the collection of data. An interesting correlation technique is suggested in a paper by Heppner (1967). For the problem at hand, the significant picture is a set of three magnetic profiles (X, Y and Z components of disturbance) along one traverse. Synchronization is important because the picture changes with time; anomalies of various types appear and disappear. Repeated viewing of a suitable movie display would give more and more understanding of the character of an electrojet in the successive stages of formation, quasi-stable interval, and dispersal. Stable intervals could be selected for analysis of the ionospheric system alone, without earth coupling or, at most, with some magnetic coupling (probably very local). Sections with different rates of time change could show different aspects of conductive earth coupling, hence providing information from the interior of the earth. The motion-picture scheme represents a full correlation and display of a vast quantity of experimental data, hence a major step towards the necessary sorting for orderly analysis.

5. In analyzing a particular anomaly, the first step is to establish the direction of current flow, assuming a long current path. This will be at right angles to the direction of the horizontal component H of magnetic disturbance; and current flow will be easterly if H is positive, westerly if H is negative. The current path is an arc of some particular radius. The main requirement is to find the direction of a radial traverse: distances on the radial traverse are analytically significant; distances on the observational traverse can be adjusted accordingly.

6. The adjusted profiles of H and Z (vertical disturbance) are equally effective for determining current strength and height of current path, or for details that would signify some compound system rather than the simple line current dealt with in most of this paper. The Z profile seems distinctly more powerful for determining the radius of curvature of the current path. It has component functions of odd and even symmetry with respect to the analytical centre. The odd function has strong character; the even function is a slow variable, roughly constant over the useful length of traverse. The even function has a marked dependence on loop radius. It is simple enough to separate the two functions in an observed profile. Their amplitude ratio signifies curvature of current path. The H profile contains a comparable pair of functions; but the curvature function is a small percentage of the whole, and therefore not easily identifiable; it becomes clear for very small loops, but other analytical techniques then apply.

7. For loops of moderately large radius, the dominant field functions observed on a spherical surface (the earth) are much like those for a simpler concept in cartesian geometry – the field of a straight-line current as observed from a flat

surface. This has two implications. One is that only part of a large current circuit is defined by a local set of observations. The radius indicated by observations is a radius of curvature for the part of the circuit within measurement range; the same real circuit observed elsewhere could show a different radius, or different height for that matter. Hence the simple circular loop used as basis for developing an analytical technique does not restrict the validity of technique in application to more realistic cases. The second important implication is that techniques already developed in cartesian geometry for cases more elaborate than the line current can be used with some validity in a spherical case. A sample given in the present study is that of a vertical current entering the ionosphere and feeding a horizontal branch; in reality the horizontal branch would be a current arc of some sort; it is treated as a straight line of semi-infinite length.

8. In the question of electromagnetic coupling of ionospheric fields with conductive, magnetic, or dielectric parts of the earth, some problems might be satisfactorily dealt with in cartesian geometry. But it would not make sense to use cartesian geometry for coupling with anything deep inside the earth, or for primary fields at much greater height than the ionosphere. A sound basis for electromagnetic analysis in spherical geometry has yet to be found. The system presented here could be developed for defining underground currents at any depth, though not for the time relationship (or phase-shift) between primary and secondary field.

Physical Outline

This paper is concerned basically with analytical methods and principles, and no specific attention is given to recorded data or to theories as to how electrojets work. Nevertheless, a brief review of the ionosphere and its current systems is appropriate. Most of it is drawn from Chapman's book, *Solar Plasma, Geomagnetism and the Aurora* (1964), and a few other references are cited.

Solar activity leads to ionization in the outer atmosphere. This produces an electrically conductive shell enveloping the earth, known as the ionosphere. Various current patterns develop in this shell, some of them closely related to auroral arcs. Solar energy provides the driving force for the currents; the earth's magnetic field is a controlling influence on their pattern. The lower atmosphere is essentially nonconductive, so that continuous vertical currents are nonexistent; but there are some arguments for current flow between the ionosphere and similar shells farther from the earth, notably the Van Allen belts.

Chapman points out that most of the conductivity of the ionosphere lies between heights of 90 and 150 kilometres above the earth's surface. Others favour a quite thin shell at a height close to 110 km. Boström (1964), citing different authors on the geometry of auroral arcs, gives a general thickness of the order of 10 km for 'homogeneous arcs', much less for 'rayed arcs'.

Chapman illustrates some typical patterns of electric current flow, in and beyond the ionosphere, for magnetically quiet days and for times of moderate and strong disturbance. All of them involve compound circulations. At times of magnetic disturbance, ionospheric currents are strongest in high latitudes and often stronger in the night hemisphere than in the sunlit hemisphere. These currents are especially concentrated along the auroral zones; and such concentrations are called the auroral electrojets. The typical boreal electrojet flows westerly in the night hemisphere, and the associated current circulation involves four loop systems. There are closures north and south of the auroral zone. There is a complementary electrojet of easterly flow in the sunlit hemisphere, with closures north and south of it. The northerly closures combined form a sort of sheet current across the polar cap.

For the main concentration (the electrojet proper) Chapman indicates currents of the order of a million amperes. With sufficient concentration, such cases might be analytically treated as simple line currents along arcs of considerable length.

Heppner (1961) discusses among other things the question of current continuity and actual closure of circuits within the ionosphere. The case is that a given electrojet may be defined as a line current for some particular length, and it must be supplied and drained at opposite ends; there is necessarily a return system, of presumably diffused current, but observational data has not yet established that the return system is entirely confined to the ionospheric shell; it might involve outer regions.

Boström (1964) develops two models of an auroral electrojet as a simple current arc of finite length in the ionosphere, fed and drained only by circuits connecting with the outer magnetosphere. In this he is mainly concerned with the sort of driving mechanism that could account for the magnitude of observed currents.

Walker (1964) gives several samples of Canadian observations and shows a high degree of correlation between auroral arcs as photographically mapped and electrojets as derived from magnetic data.

Chapman and others mention, without elaborating, the problem of electromagnetic coupling between ionospheric currents and parts of the earth itself. The problem is fundamentally important because magnetic disturbances are essentially time variations; and a time-varying electromagnetic field must involve some degree of coupling, with conductive, magnetic or dielectric parts of the earth. Coupling with major conductors – oceans or geological units – is likely to be more common than magnetic or dielectric coupling. Its general effect is to decrease the vertical intensity and increase the horizontal intensity of the magnetic field that would otherwise represent the ionospheric current system alone.

Symbols, Dimensions, etc.

Most of the basic formulae used in this work are taken from the third edition of Smythe's *Static and Dynamic Electricity* (1968). They are nearly all from Chapter 7, which is not much changed from earlier editions. Smythe consistently uses the symbol B for magnetic induction or flux density (in units of webers per square metre), and this involves a repetitious use of the symbol μ for magnetic permeability. Geophysicists usually prefer the symbol H for magnetic field intensity (in gauss or gammas). For functions expressing the same physical case, the correspondence is

$$B \text{ (in webers/metre}^2) = \frac{\mu I}{4\pi} \text{ times function}$$

$$H \text{ (in gammas)} = 100\, I \text{ times same function}$$

In both cases I is a current in amperes. The unspecified function will have a character appropriate to the case it represents; its units must be metres^{-1}.

Where Smythe is quoted in the present paper, his terms are generally used.

An amplitude that appears frequently in later developments is

$$\frac{\mu I \sqrt{1+h}}{4 \pi r}$$

in which h is a dimensionless representation of ionospheric height (relative to r). If field is measured in gammas, and if r signifies earth radius, the amplitude can be expressed

$$15.7 \times 10^{-6} \times I \sqrt{1+h}$$

For any likely height of ionospheric currents, h is roughly 0.02; so its contribution to the above expression is about one per cent. Physical amplitude is essentially proportional to current strength. The numerical amplitude of associated anomaly functions is another matter.

The symbol H, apart from its significance as a complete field intensity (vector or scalar), is used in geophysics also to specify a horizontal field component. It can be resolved into X and Y components. X, Y and Z, by geophysical convention, signify the north, east and vertical (downward) components of field; and north may signify true north, geomagnetic north, or a reference direction appropriate to a particular case. X, Y and Z are used somewhat loosely in this paper, for components of flux density, field intensity, or merely to distinguish functions regardless of their physical dimensions.

The case of the circular current loop is given by Smythe in cylindrical coordinates, z, ρ, ϕ; and the symmetry is such that ϕ appears only as the direction of current flow. For geophysical purposes, the case is transformed to spherical polar coordinates, r, θ, ϕ, with the polar axis defined as the axis of the current loop; so again ϕ appears only as the direction of current flow. The position of the loop can be specified as $r = q$, $\theta = \alpha$; so that r, θ remain free to define any point of observation. Then q represents the radius of the ionosphere. For earthbound observations, r is the radius of the earth; its mean value, $r = 6368$ km (from Clark's Tables), is quite good enough for present purposes.

The magnetic field of the current loop will naturally be strongest in the vicinity of $\theta = \alpha$. It is therefore logical to establish a local traverse parameter $\beta = \alpha - \theta$. Now β, as an angle, signifies a length normalized with respect to r. If we put $q = r(1+h)$, then h is the height of current system correspondingly normalized. Then there is no need to consider r, θ as world-wide coordinates tied to a particular current loop. They are replaced by h, β, local curvilinear coordinates appropriate to the case under observation; and the direction of β – northerly towards the centre of curvature of the current loop – is determined by purely local data.

For computing purposes, the height of ionosphere is taken to be 100 km, which leads to $h = 0.01727$. This value of h is significant mainly as a datum reference for the results of computation, i.e., Figures 3 to 9. A different choice of h would change the horizontal scale of the computed anomalies and have very little other effect. Hence, a given set of observational data can be plotted logarithmically, in the style of Figures 5 to 7, and found to fit somewhere within the appropriate set of master-curves. The position of fit then determines the height of the observed current, as well as current strength.

Analytical Considerations

Line currents and sheet currents would seem to be the obvious principal models for development. A ribbon current of arbitrary breadth is a more general model, of which the line and sheet currents are special cases. There seems to be no requirement for a slab model of any notable thickness.

The length of an auroral electrojet may be sufficiently great to be considered infinite. But there will be cases where a set of observed data must be related to end effects: the concentrated current of the electrojet is dispersed in paths confined to the ionosphere, or in paths extending upwards, or possibly both.

Developing models is strictly synthesis. But if the model is general enough analysis becomes feasible.

A complete analytical kit would involve a classification of basically different anomalies and a set of master curves, or equivalent, for each class. The simplest classification involves the geometry of the body or system giving rise to the anomaly, and the term anomaly is used to signify some field disturbance (magnetic or other) as a departure from a datum or normal value. Thus, an extensive line current in the ionosphere gives rise to an appropriately long, though not broad, magnetic anomaly at ground level; a ribbon current would have a broader anomaly; a short line current would have a locally confined anomaly; and so on. These basic distinctions are directly evident from the observational data (assuming sufficiently complete data); so there is no great difficulty in assigning a set of observations to its proper class for further analysis.

The present work represents a beginning. Circular line currents in the ionosphere constitute the principal class. Radius of loop is the variable within the class; character of anomaly changes accordingly. Height of current affects the scale rather than the character or shape of anomaly. This relationship is practically independent of loop radius; therefore height is analytically determinable. Analytical simplicity in this and other points arises from the fact that the height of the ionosphere is only a small percentage of earth radius.

For loops of reasonably large radius there is little distinction between the full development in spherical geometry and a simpler equivalent in cartesian geometry, viz., current flowing in a straight line and observed from a plane surface. An important conclusion from this is that a ribbon current, or other more general system, ought to be identifiable by analytical methods already developed in cartesian geometry.

Several cases in cartesian geometry can be found in a published paper by the present writer, Hutchison (1958). That paper deals with the anomalies of magnetized dykes and other bodies of infinite strike length. The elementary functions are mathematically identical with those required for rectilinear current flow. A dyke of vertical dip and vertical magnetization is equivalent to a ribbon current whose position and breadth correspond with the top surface of the dyke; and a very thin dyke is equivalent to a line current. Horizontal magnetic field is then represented by a solid-angle function ϕ and vertical magnetic field by a log-ratio function λ. The first vertical derivative of this anomaly – represented by the 'thin bed' class in Hutchison (1958) – is equivalent to a parallel pair of line currents with opposite sense of flow. The case for logarithmic plotting as an analytical technique is given in the same paper.

There are a good many ways of expressing the field of a circular current loop and allied cases. The present problem has been to find a satisfactory one for the case of the ionosphere. A few alternative systems and the arguments for the system chosen are reviewed here.

There is much to be said for spherical harmonic methods. Since they involve well established independent functions for the significant spherical co-ordinates r, θ there is no problem in developing current rings of any form (ribbon, sheet, slab, etc.) by integration from the initial circular line current. Even more important is the fact that spherical harmonic functions are designed for dealing with spherical boundary problems. Electromagnetic coupling can be treated as reflection at such spherical boundaries – ocean surfaces, the surface of the conductive core, or other major geologic boundaries. The weakness of spherical harmonics involves a convergence problem: there is always a critical sphere; different series expressions apply to the regions inside and outside it; neither converges satisfactorily for field points near the critical sphere. The ionosphere, as the region of primary current, is the critical sphere for the problem at hand; and the earth, as the surface of observations, has a radius only about 2 per cent less. Modern computers can cope with series of slow convergence; but for a study of character, a general expression of the case is far more satisfactory than a vast quantity of separate special calculations. A different problem, such as current systems in the outer magnetosphere and any coupling with regions deep inside the earth, would be better suited to spherical harmonic analysis. This sort of case, though with a different treatment, appears in a paper by Kendall, Chapman, Akasofu and Swartztrauber (1966). Spherical harmonic expressions for current rings, shells, etc., are given by Smythe in 7.11-13. An expression for the electromagnetic wave equation in spherical harmonics (with Bessel functions) is given by Whittaker and Watson (1927) in 18.6.

Other systems are illustrated by McNish (1938) and by Kahle and Vestine (1963), for defining ionospheric currents and for the separation of fields originating outside and inside the earth. McNish uses harmonic functions, but in cartesian geometry. Kahle and Vestine use integral expressions; but this involves integrating data over the entire surface of the earth, hardly appropriate for the study of local or regional anomalies.

A geophysical anomaly can generally be described as a wave form, but it is often an isolated wave, not part of a wave train. To represent it by the sum of numerous periodic waves (sines, cosines, etc.) is a valid method of approximation, though actually rather clumsy. McNish, in the paper cited, draws attention, with some diffidence, to an apparent earth current near a seacoast, apart from a more obvious electrojet. He is working with limited data and deriving information from a harmonic representation of it; it is not clear that the data treated directly would really show more than the electrojet.

In the present work, the expression in complete elliptic integrals for the case of a circular current loop has been taken from Smythe (7.10) after some trials with other types of development. It leads to a definition of anomalies as single-wave forms. The general expression has the great advantage of covering the full range of loop radius. One extreme is the very small loop, equivalent to a vertical magnetic dipole. The other is the straight-line current of infinite length. There is no region of mathematical failure, as there is for spherical harmonics. For field points close to the current line, one of the elliptic integrals, K, becomes highly variable, approaching infinity towards the current line. This accords with the physics of the case: magnetic field intensity approaches infinity close to the current line. But this comparison turns out to be incidental: the effect of K in the general expression actually diminishes as the current line is approached; and the physical approach to infinity is represented by a much simpler length function, of the form $1/r$.

The elliptic expression is reasonably simple to handle in the computation of anomalies. For currents in the outer magnetosphere, or at depth in the earth, it would do just as well as it does for currents in the ionosphere. The behaviour of elliptic integrals is well documented; hence the case of ribbon currents ought to be obtainable by integration of line currents, though it is not attempted here.

What is not yet clear to the present writer is whether the elliptic expression can be cast in a form suitable for the electromagnetic problem of the inonosphere with earth coupling. The significant spherical co-ordinates r, θ are mixed together in the elementary functions of the general expression. They must be separated for a satisfactory treatment of spherical boundary problems. The case calls for further investigation.

A complete electromagnetic solution, although scientifically attractive, may not actually be necessary for all analytical problems. The system so far developed should serve to identify ionospheric currents as one entity and surface or underground currents as a separate entity. From ground magnetic data there may be no way of determining the true character of the ionospheric driving signal as a function of time, and therefore no way of showing the phase shift, or equivalent time distortion, in the secondary signal. But even without this, the amplitude and geometry of the secondary field could give physical information, such as a particular conductivity beginning at a boundary of determinable depth.

Mathematical Development

The starting point is the finding of a valid mathematical description for the magnetic field of a circular-line current, an expression that remains serviceable for points of observation anywhere, and in particular for points close to the current line.

Smythe (1968) in Section 7.10 develops such an expression from first principles. The result involves the complete elliptic integrals K and E, standard functions for which tabulated values are available. Smythe works in cylindrical co-ordinates, z, ρ, ϕ, suitable to the symmetry of the case. The current loop has radius a; the origin is its centre, and the z-axis is the axis of the loop; current circulates in the ϕ-direction; the resultant magnetic field is independent of ϕ; z, ρ remain as field coordinates.

The two field components are expressed

$$B_\rho = \frac{\mu I}{2\pi} \cdot \frac{1}{R_2} \cdot \frac{z}{\rho} \left[-K + \frac{a^2+\rho^2+z^2}{{R_1}^2} E \right]$$
$$B_z = \frac{\mu I}{2\pi} \cdot \frac{1}{R_2} \left[K + \frac{a^2-\rho^2-z^2}{{R_1}^2} E \right] \tag{1}$$

Smythe's terms are here abbreviated by

$${R_1}^2 = (a-\rho)^2 + z^2$$
$${R_2}^2 = (a+\rho)^2 + z^2$$

The modulus k of the elliptic integrals is defined by

$$k^2 = 4a\,\rho/{R_2}^2$$

First, to show the validity of the general expression at points close to the current line, make the substitution

$$x = \rho - a$$

Small x and z then signify a point of observation close to the current line,

$${R_1}^2 = x^2 + z^2$$
$${R_2}^2 = 4a^2 + 4ax + x^2 + z^2$$
$$k^2 = 4a(a+x)/{R_2}^2$$

and for vanishing x and z, R_2 becomes $2a$, and $k = 1$.

Without restriction, the field components are expressible in xz coordinates.

$$B_\rho = B_x = \frac{\mu I}{2\pi} \cdot \frac{1}{R_2} \left[\frac{z}{a+x}(E-K) + 2a\frac{z}{x^2+z^2}E \right]$$
$$B_z = \frac{\mu I}{2\pi} \cdot \frac{1}{R_2} \left[K - E - 2a\frac{x}{x^2+z^2}E \right] \tag{2}$$

To let a become infinite is equivalent to letting x and z become very small without disappearing as functional parameters. In this process k approaches unity, then so does E; K approaches infinity, but it can be shown that K/R_2 vanishes. Since $2a/R_2$ approaches unity, the limiting case is

$$B_x = \frac{\mu I}{2\pi} \cdot \frac{z}{x^2+z^2}$$
$$B_z = \frac{\mu I}{2\pi} \cdot \frac{-x}{x^2+z^2} \tag{3}$$

This is the field of a y-directed straight-line current of infinite length.

The disposal of K involves its appropriate series expansion in $1-k^2$, which can be found in Jahnke and Emde (1945), Section V. 13. It is easy enough to see that $1-k^2 = (R_1/R_2)^2$ without restriction. The initial term of the series is then $\lambda = \ln(4R_2/R_1)$. By l'Hôpital's rule $(\ln R_2)/R_2$ vanishes for infinite R_2. The other terms vanish more obviously.

It is also worth nothing that the general expression is simplified for loops of very small radius. Small a implies small k. Appropriate series expansions for K and E can be found in Jahnke and Emde, Section V. 12. The elimination of ρ is no longer appropriate. The two lengths R_1 and R_2 always signify the distance from field point to the nearest and farthest points of the current loop. For small loops they become roughly equal and can be approximated by a single length

$$R^2 = \rho^2 + z^2$$

The full development for small loops is elaborate, and it is not given here. It results in series beginning with the well known dipole functions

$$B_\rho = \frac{\mu I a^2}{4} \cdot \frac{3\rho z}{R^5}$$
$$B_z = \frac{\mu I a^2}{4} \cdot \frac{2z^2 - \rho^2}{R^5} \tag{4}$$

and continuing with terms containing successive odd powers of $1/R$. In a rigorous treatment, R_1 and R_2 remain distinct; their combined powers represent the same sequence.

It will be noted that loop area, represented by a^2, is a significant part of the governing amplitude for small loops. For large loops it is not.

The main object of this chapter is to show how the initial field equations are transformed to spherical coordinates appropriate to the ionospheric problem. Pictures help, and Figures 1 and 2 are perhaps easier to follow than words.

Figure 1 shows the cylindrical coordinate system for Equations (1) and the supplementary x introduced for

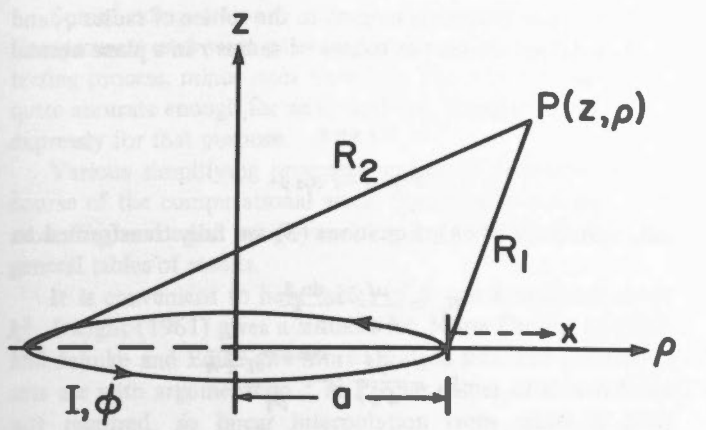

FIGURE 1. Cylindrical coordinate system.

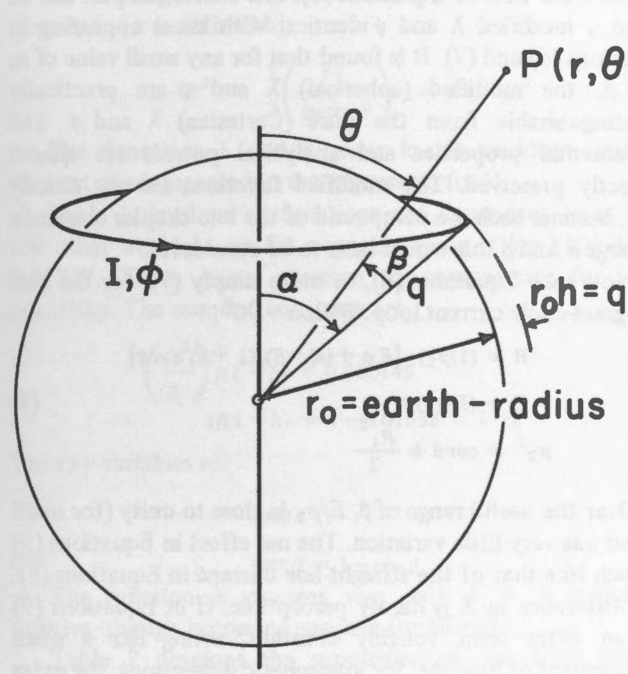

FIGURE 2. Spherical polar coordinate system.

Equations (2) and (3). Figure 2 shows the transformation to spherical polar coordinates of the same axis but different origin.

In Figure 2 the origin is the centre of the earth. The polar axis has nothing to do with geographic or geomagnetic coordinate systems; it signifies purely the axis of the current loop. The loop lies in a spherical surface of radius q; and it has a size defined by the polar angle α; so

$$a = q \sin\alpha$$

The field point P can be anywhere, with coordinates r, θ; then

$$z = r\cos\theta - q\cos\alpha$$

$$\rho = r\sin\theta$$

or

$$x = r\sin\theta - q\sin\alpha$$

The required field components are radial and tangential to the sphere through P; so

$$B_r = B_x \sin\theta + B_z \cos\theta$$
$$B_\theta = B_x \cos\theta - B_z \sin\theta$$

The general case, from Equations (1) or (2), is then, in spherical coordinates,

$$B_r = +\frac{\mu I}{2\pi}\cdot\frac{1}{R_2}\left[\frac{q}{R}\cos\alpha\,(K-E) + 2q^2\,\frac{\sin\alpha\sin(\alpha-\theta)}{R_1^{\,2}}\,E\right]$$

$$B_\theta = -\frac{\mu I}{2\pi}\cdot\frac{1}{R_2}\left[\frac{r - q\cos\alpha\cos\theta}{r\sin\theta}(K-E) + \frac{2q\sin\alpha\left\{q\cos(\alpha-\theta) - r\right\}}{R_1^{\,2}}\,E\right] \tag{5}$$

and, in Equations (5),

$$R_1^{\,2} = r^2 + q^2 - 2rq\cos(\alpha-\theta)$$
$$R_2^{\,2} = r^2 + q^2 - 2rq\cos(\alpha+\theta)$$
$$k^2 = 4rq\sin\alpha\sin\theta/R_2^{\,2}$$

or $\quad 1 - k^2 = R_1^{\,2}/R_2^{\,2} \quad$ as always.

The particular case under investigation concerns field observations at the surface of the earth. With reference to Figure 2, it is convenient to define this surface by $r = r_o$.

The polar angles α and θ can be regarded as surface lengths normalized with respect to r_o. The angle $(\alpha - \theta)$ appears repeatedly; so it is replaced by a local curvilinear coordinate

$$\beta = \alpha - \theta$$

The height of the ionosphere above the earth is $q - r_o$. Put

$$h = (q - r_o)/r_o$$

and h is a normalized length in the same measure as β (both are dimensionless). Now β, h are an orthogonal pair of local coordinates appropriate to a ϕ-directed line current; they are counterparts of x,z in Equations (3).

In the further transformation of Equations (5) to local coordinates, several items can be reduced to simpler form; some new symbols are introduced; r, without subscript, signifies earth radius. A few explanatory statements lead on to the next pair of field equations.

$$R_1^{\,2} = r^2\left[2(1+h)(1-\cos\beta) + h^2\right]$$
$$= 2r^2(1+h)\,p_1^{\,2}$$
$$p_1^{\,2} = \frac{h^2}{2(1+h)} + 1 - \cos\beta$$
$$R_2^{\,2} = r^2\left[2(1+h)\left\{1 - \cos(2\alpha-\beta)\right\} + h^2\right]$$
$$= 4r^2\sin^2\alpha\,(1+h)\,p_2^{\,2}$$
$$p_2^{\,2} = \cos\beta - \sin\beta\cot\alpha + p_1^{\,2}/2\sin^2\alpha$$

This expression for p_2 is convenient in computations as long as $\sin\alpha$ is moderately large in terms of h. However, the main reason for it is to clear $2q^2 \sin\alpha$ out of the last terms of Equations (5). Those last terms contain the most significant elementary functions,

$$\lambda = \frac{\sin\beta}{p_1^{\,2}}$$

$$\phi = \frac{\cos\beta - \dfrac{1}{1+h}}{p_1^{\,2}}$$

These two functions are totally independent of α; and they are perfect transfomations of the xz functions in Equations (3).

The final transformation to local coordinates is then

$$B_r = \frac{\mu I\sqrt{1+h}}{4\pi r}\cdot\frac{1}{p_2}\left[(K-E)\cot\alpha + E\lambda\right]$$

$$-B_\theta = \frac{\mu I\sqrt{1+h}}{4\pi r}\cdot\frac{1}{p_2}\left[(K-E)\left\{1-\frac{\cos\beta-\dfrac{1}{1+h}}{\sin\alpha\sin(\alpha-\beta)}\right\}+E\phi\right]$$

with

$$1-k^2 = \frac{1}{2}\left(\frac{p_1}{p_2\sin\alpha}\right)^2 = (R_1/R_2)^2 \qquad (6)$$

Further comments concern the character of these expressions as functions of β and h.

By geophysical convention, Z is a vertical field component, positive downwards, and H the complete horizontal component, positive northerly; in other words, Z and H represent negative r and θ components. Current flow is easterly in the present development. It is now convenient to use Z and H for the functional parts of Equations (6) without physical amplitude; so

$$\mathrm{H} = (1/p_2)\left[E\phi + (K-E)\left\{1-\frac{\cos\beta-\dfrac{1}{1+h}}{\sin\alpha\sin(\alpha-\beta)}\right\}\right]$$

$$-\mathrm{Z} = (1/p_2)\;[E\lambda + (K-E)\cot\alpha] \qquad (7)$$

These functions have a numerical amplitude, dependent mainly on the value of h; there is a contribution for α, but it is minor except for very small α. As β varies, the curve or profile described by H or Z has much the same shape for any α (unless α is very small); but the horizontal scale of profile is directly dependent on the value of h. Thus, for a reasonably large loop, h can be determined from the scale of an observed profile.

Much of the analytical power is in the elementary functions λ and ϕ. The two symbols are taken from a paper by Hutchison (1958); the complete λ and ϕ are a pair of functions which, among other things, exactly described the field of a ribbon current; the line current is the particular ribbon of zero breadth.

In Equations (3) λ and ϕ appear in pure form, to describe the field of a y-directed line current of infinite length; viz.,

$$\lambda = -x/(x^2+z^2)$$

$$\phi = z/(x^2+z^2)$$

If this line current is tangent to the sphere of radius q, and if observations are on the sphere of radius r in a plane normal to y, then

$$x = r\sin\beta$$

$$z = q - r\cos\beta$$

and, with $q = r(1+h)$, Equations (3) are fully transformed to

$$B_r = \frac{\mu I}{4\pi r}\cdot\frac{\sin\beta}{p_1^{\,2}}$$

$$-B_\theta = \frac{\mu I}{4\pi r}\cdot\frac{\cos\beta-\dfrac{1}{1+h}}{p_1^{\,2}} \qquad (8)$$

The physical amplitude here differs only by a factor of $\sqrt{1+h}$ from that of Equations (6). The functional part can be called a modified λ and ϕ identical with those appearing in Equations (6) and (7). It is found that for any small value of κ, and β, the modified (spherical) λ and ϕ are practically indistinguishable from the pure (Cartesian) λ and ϕ. The fundamental properties and analytical powers are almost perfectly preserved. The modified functions are not strictly pure, because each is a compound of the two simpler elements; for large h and β this would have to be considered.

Now take Equations (6), or more simply (7), for the case of a great-circle current loop. With $\alpha = 90°$,

$$\mathrm{H} = (1/p_2)\;[E\phi + (K-E)/(1+h)\cos\beta]$$

$$-\mathrm{Z} = (E/p_2)\,\lambda \qquad (9)$$

and $$p_2^{\,2} = \cos\beta + \frac{p_1^{\,2}}{2}$$

Over the useful range of β, E/p_2 is close to unity (for small h) and has very little variation. The net effect in Equations (9) is much like that of the straight-line current in Equations (8). The difference in Z is hardly perceptible. H in Equations (9) has an extra term, roughly constant, acting like a small displacement of baseline; for ionospheric dimensions, the extra term adds a little less than 5 per cent to the H amplitude.

For the great-circle case, p_2, K, E, and the function attached to $(K-E)$ all have perfect, even symmetry with respect to β. For smaller $\sin\alpha$, they are all functions involving θ, i.e., $\alpha-\beta$; and they have no simple symmetry with respect to β.

It is analytically useful to express the general case in functions having odd and even symmetry in β. This could be done albegraically; but it is just as practical to compute from Equations (7) over a suitable range of positive and negative β, and then resolve the results.

Computation, Tables

The computations done in the present project have been essentially for test purposes, to find out the behaviour of Equations (7) and other more special cases. They lead to a more or less complete set of master curves for Equations (7), though the set could be improved.

Some computational errors showed up in plotting. Conspicuous ones were examined and corrected as part of the testing process; minor ones were left. The results are probably quite accurate enough for analytical use, though not developed expressly for that purpose.

Various simplifying processes suggested themselves in the course of the computational work. Some comments are worth recording, and some sample workings are given, apart from the general tables of results.

It is convenient to have tables of K and E with argument k^2. Dwight (1961) gives a suitable set. Milne-Thomson (1950) and Jahnke and Emde give more abridged sets. The commoner sets are with argument $\sin^{-1} k$. Precise values of K and E are not required, so linear interpolation from tables is good enough.

In working from Equations (7), p_1 and p_2 are both required, and k is defined by

$$1-k^2 = \frac{1}{2}\left(\frac{p_1}{p_2 \sin \alpha}\right)^2 = (R_1/R_2)^2$$

The functions λ and ϕ occur in all workings, and an element of φ is repeated in the expression for H.

Table 1 develops all functions not dependent on α. This and other workings are for a specific value of $h = 110/6368 = 0.01727$. There is no occasion to approximate for small quantities. The required constants are

$$\left(\frac{h^2}{2}\right)/(1+h) = 0.000146$$

$$1/(1+h) = 1-0.01698 = 1-g$$

The key variables are

$$\sin \beta$$

and

$$\operatorname{vers} \beta = 1 - \cos \beta$$

The function λ changes sign with β; ϕ is essentially positive, though becoming negative for $|\beta|>10°$.

Table 2 develops the supplementary functions for the great-circle current loop ($\alpha = 90°$). This shows K with its highest value for any case with the same h. It is convenient to abbreviate part of Equation (9) for H by

$$\delta = (K-E)/E(1+h)\cos\beta$$

so that E/p_2 multiplied by λ or $(\phi + \delta)$ gives the field functions.

Table 2 is overdeveloped in that δ to the first decimal place would be good enough, and so δ is practically the same as (K-E), or (K-1); also, the variation in E/p_2 could be disregarded as it affects only the weakest parts of the final anomaly. But in cases of smaller α the supplementary functions have more variation and play a stronger part in the end product.

Table 3 gives the field functions for the great-circle case, derived from Tables 1 and 2. The higher values of H, though recorded to four figures, should actually be rounded off to three, because they contain a $p_1{}^2$ determined to only three significant figures. Note that H, unlike ϕ, has no change of sign. Its only zeros are at the poles $\alpha - \beta = \theta = 0, \pi$.

Table 1. Basic Functions

β	$p_1{}^2$	$\sin\beta$	$g - \operatorname{vers}\beta$	λ	ϕ
° ′					
0	0.000 146	0	0.016 98	0	116.3
6	148	0.001 745	0.016 98	11.8	114.7
12	152	3 491	97	23.0	111.7
24	170	6 981	95	41.1	99.7
36	200	10 472	92	52.4	84.6
48	243	13 962	88	57.5	69.5
1 00	0.000 298	0.017 45	0.016 82	58.6	56.4
1 12	365	20 94	76	57.4	45.9
1 30	489	26 18	63	53.5	34.0
2 00	755	34 90	37	46.2	21.7
3	0.001 516	0.052 34	0.015 61	34.5	10.30
5	3 951	87 16	13 17	22.1	3.33
7	7 600	121 87	9 52	16.0	1.25
10	0.015 338	0.173 65	0.001 785	11.32	0.116
15	0.034 222	0.258 8	−0.017 10	7.56	−0.500

Table 2. Supplementary Functions (α = 90°)

β	$p_2{}^2-1$	$1-k^2$	K	E	δ	E/p_2
° ′						
0	+0.000 073	0.000 073	6.15	1.00	5.06	1.000
12	070	076	6.12		5.03	
36	045	100	6.00		4.92	
48	+0.000 025	121	5.90		4.82	
1 00	− 0.000 003	0.000 149	5.79	1.00	4.71	1.000 5
12	036	183	5.69		4.61	1.001
30	098	245	5.54		4.46	
2 00	232	378	5.33		4.26	1.001
3	− 0.000 612	0.000 758	4.98	1.00	3.91	1.002
5	1 830	1 978	4.50		3.44	1.005
7	3 654	3 814	4.17	1.01	3.12	1.009
10	− 0.007 523	0.007 727	3.82	1.01	2.77	1.020
15	− 0.016 963	0.017 400	3.42	1.02	2.38	1.034

Table 3. α = 90°

β	$\phi + \delta$	H	−Z
° ′			
0	121.4	121,4	0
6	119.8	119.8	11.8
12	116.7	116.7	23.0
24	104.7	104.7	41.1
36	89.5	89.5	52.4
48	74.3	74.3	57.5
1 00	61.1	61.1	58.6
1 12	50.5	50.5	57.4
1 30	38.5	38.5	53.6
2 00	26.0	26.0	46.3
3	14.21	14.24	34.6
5	6.77	6.80	22.2
7	4.37	4.41	16.2
10	2.89	2.95	11.55
15	1.88	1.94	7.82

The remaining tables give only the end results of computation, cast in a form for logarithmic plotting. H(β) is expressed as the sum of a primary function not changing sign with β, and a secondary function that does change sign with β and carries the sign appropriate to positive β. For the smaller

Table 4. H for various α

$\alpha =$	45°	30°	15°	7°	1°24′
(β°)					
0.00	120.5 + 0	120.0 + 0	118.8 +0	116.0 + 0	84.8 + 0
0.2		116	115 +0.5	112.2 + 1.2	81.5 + 3.0
0.6	89.0 + 0.1	88.6 + 0.8	87.6 +1.8	84.8 + 3.4	56.8 + 4.0
1.0	60.8 + 0.6	60.3 + 0.9	59.2 +1.9	56.4 + 4.1	30.1 − 0.6
1.5	38.5 + 0.5	37.6 + 0.85	36.8 +1.9	34.6 + 3.1	4.1 − 11.5
2.0	25.6 + 0.4	25.2 + 0.7	24.2 +1.7	22.4 + 2.6	−18.5 − 26.9
3	13.8 + 0.3	13.4 + 0.6	12.6 +1.3	10.9 + 1.6	−37.2 − 41.3
5	6.4 + 0.2	6.0 + 0.4	5.2 +0.9	3.5 + 0.3	− 3.4 − 4.1
7	4.0 + 0.2	3.7 + 0.3	2.9 +0.6	0.8 − 0.8	− 0.6 − 0.9
10	2.6 + 0.1	2.2 + 0.1	1.4 +0.2	− 3.1 − 3.8	

Table 5. $-Z$ for various α

$\alpha =$	45°	30°	15°	7°	1°24′
(β°)					
0.0	4.8 + 0	7.7 + 0	14.2 +0	24.7 +0	55.1 +0
0.2	4.8 + 23.0	7.7 + 23.0	14.3 +23.1	24.8 +23.3	55.8 +25.2
0.6	4.9 + 52.4	7.9 + 52.4	14.6 +52.6	25.7 +53.5	60.3 +60.5
1.0	5.0 + 58.6	8.0 + 58.7	14.8 +59.1	25.6 +60.8	64.8 +72.8
1.5	4.9 + 53.9	7.9 + 53.8	14.6 +54.4	25.9 +56.5	66.0 +74.2
2.0	4.8 + 46.3	7.7 + 46.5	14.4 +47.2	25.0 +50.1	62.7 +68.7
3	4.6 + 34.7	7.4 + 34.9	13.4 +36.1	23.8 +40.2	13.6 +17.0
5	4.1 + 22.4	6.6 + 22.7	12.1 +24.3	22.5 +30.2	−3.4 − 2.0
7	3.8 + 16.4	6.0 + 16.8	11.3 +18.9	22.6 +27.2	−1.3 − 0.7
10	3.5 + 11.9	5.1 + 12.0	10.6 +15.0	27.1 +29.7	

loops there are further changes of sign, because the range of β is carried through a pole of the loop. $Z(\beta)$ is expressed in the same manner, though the part not changing sign with β is normally the weaker function.

To reduce crowding, the first column is put in degrees and tenths instead of degrees and minutes.

Special Cases

Small current loops, current circuits not confined to the ionosphere, and a few particular aspects of the general current loop are treated separately.

Small Loops

In the general case of circular current loops, it has been shown that loop radius has only a minor effect on the amplitude and essential shape of the magnetic anomaly – until the radius approaches its zero-limit. From the observational point of view the anomaly of a small loop is locally confined and therefore not easily mapped. For analytical purposes the pole of the loop is the best centre of symmetry.

Equations (4) in the mathematical development define the anomaly of a loop of infinitesimal radius, in cylindrical co-ordinates. Transformation to spherical co-ordinates is hardly necessary for practical purposes, but is recorded here in a form comparable to Equations (6)

$$B_r = \frac{\mu I \sqrt{1+h}}{4\pi r} \cdot \frac{\pi \sin^2 \alpha}{\sqrt{2}} \cdot \frac{p_1^{\,2} \cos\theta - 3/4(\sin^2\theta)}{p_1^{\,5}}$$

$$-B_\theta = \text{“} \quad \cdot \quad \text{“} \quad \cdot \frac{\sin\theta\,(3h - h^2 + \operatorname{vers}\theta)}{4 p_1^{\,5}}$$

in which p_1 is the same as before; for this case $\cos\theta = \cos\beta$; but there is no reason to use β.

These dipole functions are shown as dotted lines in Figures 3 and 4. A specific value $\alpha = 0°24'$ is chosen for two reasons; $\sin^2\alpha$ controls the amplitude of the dipole anomaly; and the true centre of the anomaly must be at $\beta = \alpha$ for comparison with the other cases illustrated.

Dipole functions have no place in the scheme of Figures 5 and 6. In Figure 7 they are shown again, logarithmically plotted; and the same figures gives a normalized $H(\theta)$ and $Z(\theta)$ for the case $\alpha = 1°24'$.

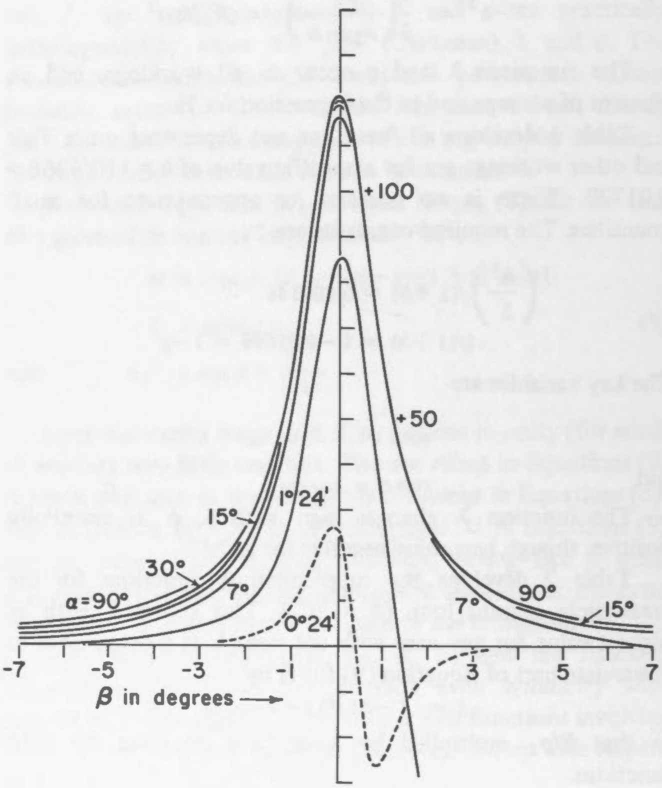

FIGURE 3 – HORIZONTAL COMPONENT. The curves represent Equations (7) for H, as developed in Table 4. The parameter of traverse distance is β, here scaled in degrees: length equivalents are 100 km = 0.9°; 100 miles = 1.15°. The radius of each loop is represented by a polar angle α. The true (plane) radius is 6478 km sin α. The curves have numerical amplitudes. Their physical amplitudes would be these values multiplied by $\mu I\sqrt{.1+h}\,/4\pi r$ (for flux density in webers/metre^2) or by $100\, I\sqrt{1+h}\,/r$ (for field intensity in gammas). As α ranges from 90° down to 7° there is not much change in amplitude or character. Note that for $\alpha = 7°$ the axial centre of the loop is at the right-hand edge of the diagram; H there passes through zero and describes a negative image of the part illustrated. So also for the smaller loops. The broken curve is purely a dipole function, an imperfect representation of the case $\alpha = 0°24'$.

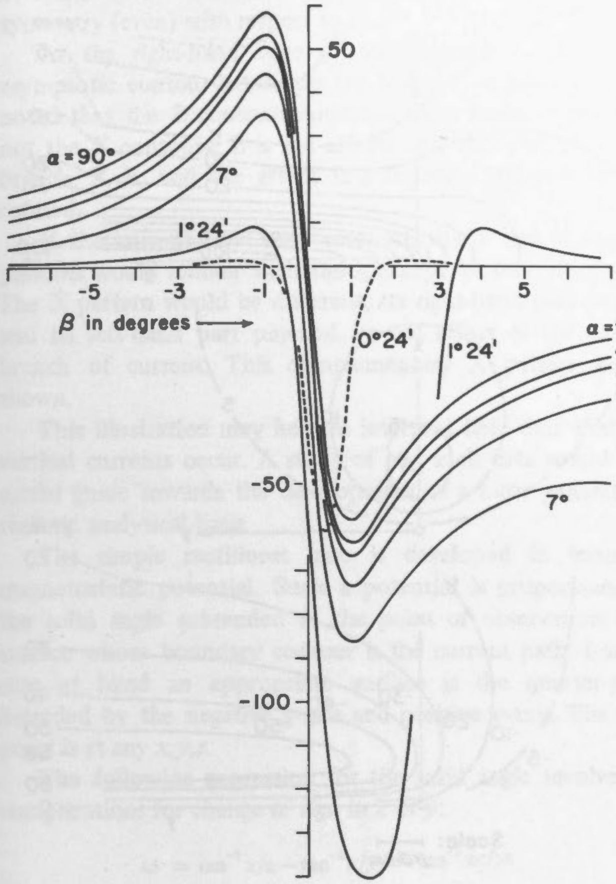

FIGURE 4 – VERTICAL COMPONENT. The curves represent Equation (7) for Z, as developed in Table 5. The scheme is the same as that of Figure 3. As α ranges from 90° down to 7° the chief effect is a downward shift of curves; there is not much other change in amplitude or character. Again for $\alpha = 7°$ the axial centre is at the right-hand edge; but Z here reflects itself, developing another negative peak before recrossing the zero-line and fading out. For $\alpha = 1°24'$, Z has a single flattish negative extreme, instead of a pair. For smaller loops, this flatness and the total breadth of the anomaly diminish to the dipole limit. The broken curve is a dipole function, as before, with the same arbitrary choice of α.

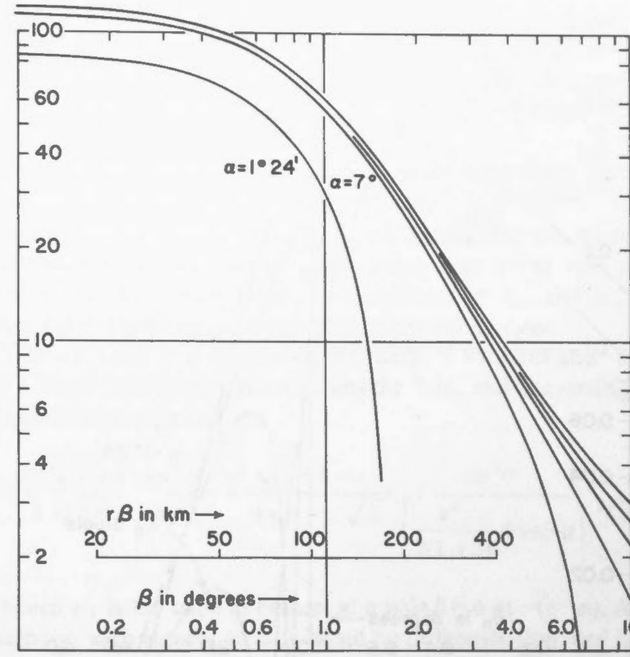

FIGURE 5 – HORIZONTAL COMPONENT, LOGARITHMIC. The curves represent H averaged for positive and negative β. They are functions of even symmetry with respect to β, the first entries in Table 4. The corresponding curve for a straight-line current observed from a plane would lie between the curves for $\alpha = 7°$ and $\alpha = 15°$. Negative parts of the curves for $\alpha = 1°24'$ and 7° are not shown. The zero crossings occur slightly beyond $\beta = \alpha$. A full treatment would show also the functions of odd symmetry given in Table 4; but those functions are not considered analytically useful, and only for α less than 30° are they strong enough to appear in the diagram. The curve for $\alpha = 1°24'$ is not particularly significant in this scheme. For small loops the more suitable analytical centre is at $\beta = \alpha$ (i.e., $\theta = 0$).

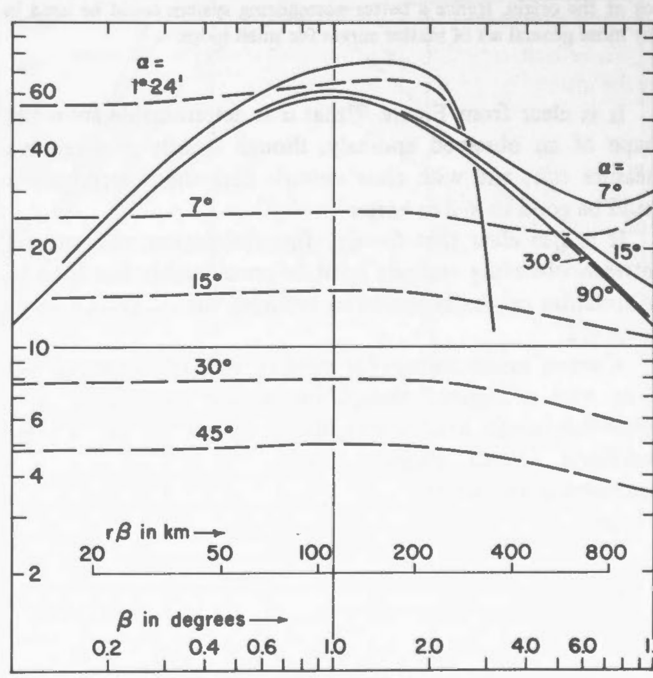

FIGURE 6 – VERTICAL COMPONENT, LOGARITHMIC. The curves represent the two parts of Z given in Table 5, having odd and even symmetry with respect to β – odd symmetry in solid line, even symmetry in dashed line. There is no component of even symmetry for $\alpha = 90°$. The corresponding curve for a straight-line current observed from a plane is hardly distinguishable from the curve for $\alpha = 90°$. The point of most interest for analysis is that the odd functions have a shape practically independent of α, except for quite small α; and the even functions are practically independent of β, though with relative amplitude clearly dependent on α. Hence, observed data can be readily resolved into odd and even components, and the ratio of their amplitudes then determines α. The even functions appear again as $Z_0(\alpha)$ in Figure 9.

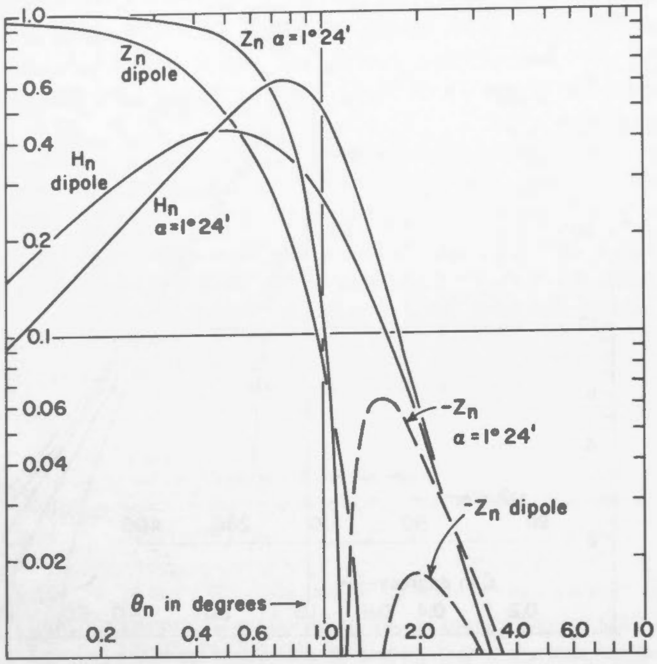

FIGURE 7 – SMALL LOOPS, LOGARITHMIC. Normalized field components H_n and Z_n are shown as functions of θ or θ_n, for the small loop ($\alpha = 1^\circ 24'$) and the infinitesimal loop, or vertical dipole. H_n and Z_n represent $H(\theta)$ and $Z(\theta)$ both divided by $Z(0)$. The traverse parameter is θ for the dipole and $\theta/1.74$ for the other loop. Dimensions are thus normalized, arbitrarily, for a clearer comparison of shapes. Z_n has unit value at the origin, diminishes to a zero-crossing for θ_n between 1° and $1\ 1/2^\circ$, has a negative peak for θ_n between $1\ 1/2^\circ$ and 2°, and then fades out at roughly a third-power rate. The negative peak becomes stronger and moves closer to the origin as α increases. H_n is zero at the origin, has a peak for θ_n between $1/2^\circ$ and 1°, then fades out at nearly a fourth-power rate. The peak becomes stronger and moves farther from the origin as α increases. For α greater than $1^\circ 24'$, maximum Z is not at the origin. Hence a better normalizing system could be used in any more general set of master curves for small loops.

It is clear from Figure 7 that α is determinable from the shape of an observed anomaly, though strictly in a relative measure α/h; and with clear enough data the determination could be good to $h/2$ or better.

It is also clear that for any fine distinction, the interval between observing stations must be considerably less than h: information can be improved by reducing the interval down to about $h/5$.

A set of master curves for small loops could be developed in the style of Figure 7, though a better system of normalizing might be used. For a roughly comparable example see Hutchison (1958) Figure 4 – other functions, actually representing an antiparallel pair of line currents, in Cartesian geometry.

Vertical Current

If ionospheric current systems are fed or drained by circuits extending outwards, there must be some appropriate magnetic effect observable on the earth. Identification might be difficult if the current entering or leaving is more diffused

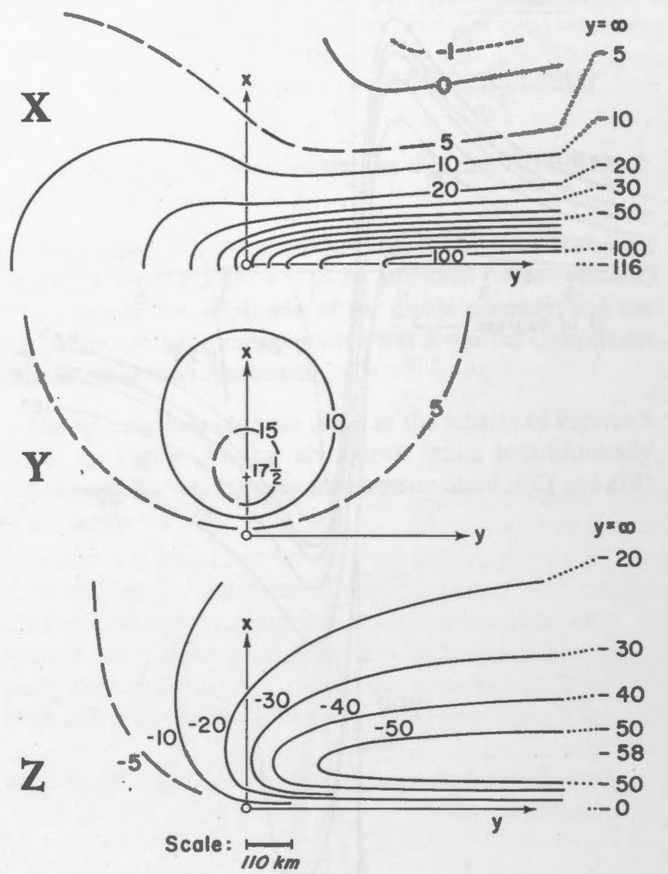

FIGURE 8 – VERTICAL CURRENT. Contour patterns are shown for the three Cartesian components of magnetic field. The anomaly represents a line current of two straight branches. Current I flows down the z-axis to the origin (in the ionosphere), then along the y-axis (considered positive easterly). Mapping is in the plane $z = h$, i.e., below the current system and normal to the vertical branch. All three contour patterns have simple symmetry with respect to $x = 0$, so the northerly half is a sufficient illustration of each. X is essentially positive in both halves. Y is positive in the north half, negative in the south half. Z is negative in the north half, positive in the south half. The horizontal scale and field units in this figure are the same as in Figures 3 and 4 – the scale not precisely the same, as a length unit of 110 km is used here instead of one degree of geographical arc (111 km).

than the ionospheric part of the circuit. A clear and simple case is expressed by a single line current with vertical and horizontal branches.

In the sample given here it is assumed that a line current (of intensity I) enters the ionosphere vertically, then flows easterly in a large arc. The essential effect can be shown in Cartesian geometry, which much simplifies the work.

Figure 8 shows contour patterns for the X, Y and Z components of magnetic field. Current flow is down the negative half of the z-axis to an origin in the ionosphere, then along the positive half of the y-axis; the x-axis is considered positive northerly. There is complete symmetry in the yz plane; and so only the north half of each contour pattern is shown. The X component has even symmetry with respect to

x; Y and Z have odd symmetry with respect to x; Y alone has symmetry (even) with respect to y.

At the right-hand edge of the diagram are shown the asymptotic contour intercepts for X and Z at infinite y. It is noted that the Z contours approach these limits rapidly, but not the X contours: Z is not affected by the vertical current branch, X is, and the effect is a function identical with Y rotated.

If the current flow were reversed, the Y and Z contour patterns would remain unchanged, except for reversal of signs. The X pattern would be different, its right-hand part swollen and its left-hand part pinched, as the effect of the vertical branch of current. This complementary X pattern is not shown.

This illustration may help to interpret field data if strong vertical currents occur. A study of any such data would be a useful guide towards the development of a more general and realistic analytical basis.

The simple rectilinear case is developed in terms of magnetostatic potential. Such a potential is proportional to the solid angle subtended at the point of observation by a surface whose boundary contour is the current path. For the case at hand an appropriate surface is the quarter-plane bounded by the negative z-axis and positive y-axis. The field point is at any x,y,z.

The following expression for the solid angle involves no complications for change of sign in x or y:

$$\omega = \tan^{-1} x/z - \tan^{-1} x/y + \tan^{-1} xc/yz$$

with $$c^2 = x^2 + y^2 + z^2$$

The x, y and z derivatives of ω then represent the components of magnetic field. They can be normalized with respect to the height z and tidily grouped. Let $z = h$, $x = uh$, $y = vh$, and $c = bh$; so $b_2 = 1 + u^2 + v^2$. Then

$$X = \frac{1}{h}\left[\frac{1}{1+u^2}\left(1+\frac{v}{b}\right) - \frac{v}{u^2+v^2}\left(1-\frac{1}{b}\right)\right]$$

$$Y = \frac{1}{h} - \frac{u}{u^2+v^2}\left(1-\frac{1}{b}\right)$$

$$Z = -\frac{1}{h}\cdot\frac{u}{1+u^2}\left(1+\frac{v}{b}\right)$$

Note that as v becomes negatively infinite, all functions vanish; and as v becomes positively infinite, $1 + v/b = 2$, and all other v functions vanish. The latter case gives the standard case of an infinitely long straight-line current. From Equations (3), or Smythe 7.14, the physical amplitude for X, Y and Z must then be $\mu I/4\pi$; and if h is a proportion of earth-radius, as elsewhere in this paper, the physical amplitude is $\mu I/4\pi r$.

Miscellaneous

A few characteristics of the circular loop are reviewed as functions of α.

The value of $-Z$ at $\beta = 0$ can be falled Z_0; and it is significant for determining α. A curve of $Z_0(\alpha)$ is therefore a useful supplement to the curves of Figure 6. Z_0 is mainly significant of $Z(\beta)$; let this be called Z_m. Now $H_0(\alpha)$ is a simpler determination than $Z_m(\alpha)$, and it can be used as a reference amplitude for $Z_0(\alpha)$, hence as a rough substitute for $Z_m(\alpha)$.

Logarithmic curves for Z_0 and H_0, as α ranges from 6′ to 90°, are shown in Figure 9. The full range of α extends to 180°; Z_0 has opposite sign in the lower hemisphere. But when α is within a few degrees of either polar value (0 or 180°), there is no particular point to the curves of Z_0 and H_0, because $\beta = 0$ is no longer a practical centre for analysis.

On the polar axis of any circular loop, H vanishes and $-Z$ has a simple expression, given in Smythe 7.10, and convertible to spherical coordinates as

$$B_r = \frac{\mu I\sqrt{1+h}}{4\sqrt{2r}}\cdot\frac{\sin^2\alpha}{p_1^{\,3}} = \frac{\mu I\sqrt{1+h}}{4\pi r}\cdot\frac{\pi}{\sqrt{2}}\cdot\frac{\sin^2\alpha}{\left\{\dfrac{h^2}{2(1+h)} + \operatorname{vers}\alpha\right\}^{3/2}}$$

in which p_1 is the same as before: at a pole $\beta = \alpha$ or $-(\pi-\alpha)$. A maximum with respect to α is found by differentiation; and it occurs when α is a little less than 1° 24′. This is the reason for including that value in the general computations. The axial or polar field function can be expressed, for conformity, as

$$Z_p(\alpha) = -\frac{\pi}{\sqrt{2}}\,(\sin^2\alpha)/p_1^{\,3}$$

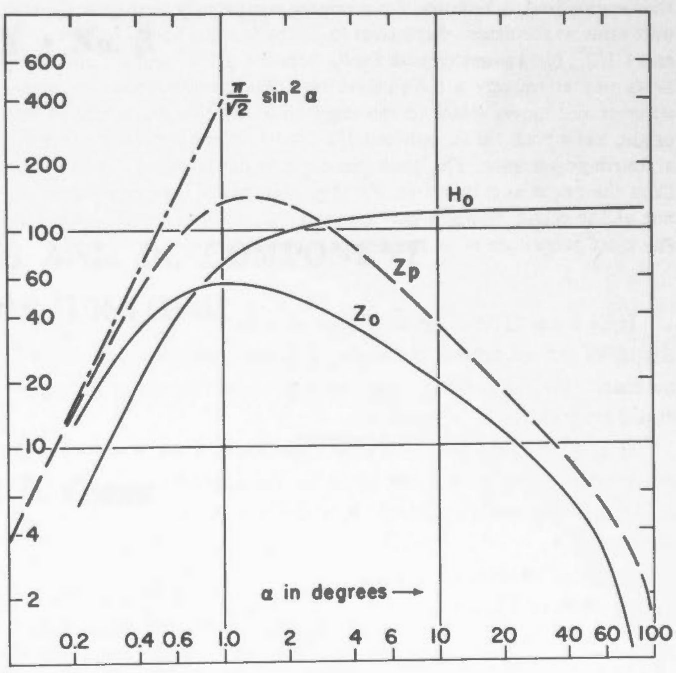

FIGURE 9 – LOOP FUNCTIONS WITH ARGUMENT α. These logarithmic curves show the miscellaneous functions discussed under Special Cases, Miscellaneous. H_0 and Z_0 are field values at $\beta = 0$, amplitudes of Figures 5 and 6 more fully displayed. The power of Z_0 for determining α is here more clearly seen. Z_p represents total field at the pole of a loop. For small α it becomes asymptotic to $(\pi/\sqrt{2})\sin^2\alpha$, a dipolar amplitude which appears in Special Cases, Small Loops, and is used for the dipolar curves in Figures 3 and 4.

For small α, Z_p varies as $\sin^2\alpha$ and thus represents the amplitude of a dipolar anomaly. But the pure dipolar amplitude does not contain vers α in its denominator and is therefore greater than Z_p. The difference is negligible up to about $\alpha = 12'$. For $\alpha = 24'$ the dipolar expression gives an amplitude about 20 per cent too high; it is a reasonable guess that the fully developed anomaly for a loop of this radius would have a shape detectably different from the dipolar anomaly; in other words, the dipolar curves in Figures 3 and 4 are only a rough picture of the case they represent.

The curve of Z_p is shown in Figure 9. It has no very practical significance for α greater than a few degrees. Its general characteristics are that axial field increases as loop size increases, up to a point, and then decreases because the loop is effectively farther from the point of observation; then, as α approaches 90° the growth in loop size slows down and reverses, so that field intensity falls off more rapidly, finally vanishing at $\alpha = 180°$.

References

Boström, Rolf, 1964. A model of the auroral electrojets. *J. Geophys. Res.*, 69, 4983-4999.

Chapman, S., 1964. Solar plasma, geomagnetism and aurora. *Documents on Modern Physics.* Gordon and Breach.

Dwight, Herbert Bristol, 1961. *Mathematical Tables*, third ed. Dover.

Heppner, J.P., 1967. High latitude magnetic disturbances (A brief review with initial results from motion picture presentation). In *Aurora and Airglow*, ed. by Billy M. McCormac, Reinhold Publ. Corp. New York, pp. 75-92.

Hutchison, Ralph D., 1958. Magnetic analysis by logarithmic curves. *Geophysics*, 23, 749-769.

Jahnke, Eugene, and Emde, Fritz, 1945. *Tables of Functions*, fourth ed. Dover.

Kahle, A.B., and Vestine, E.H., 1963. Analysis of surface magnetic fields by integrals. *J. Geophys. Res.*, 68, 5505-5515.

Kendall, P.C., Chapman, S., Akasofu, S.-I., and Swartztrauber, P.N., 1966. The computation of the magnetic field of any axisymmetric current distribution – with magnetospheric applications. *Geophys. J.*, 11, 349-364.

McNish, A.G., 1938. Heights of electric currents near the auroral zone. *Terr. Mag. and Elect.*, 43, 67-75.

Milne-Thomson, L.M., 1950. *Jacobian Elliptic Function Tables.* Dover.

Smythe, William R., 1968. *Static and Dynamic Electricity*, third ed. McGraw-Hill.

Walker, J.K., 1964. Space-time associations of the aurora and magnetic disturbances. *J. Atmos. and Terresst. Phys.*, 26, 951-958.

Whittaker, E.T., and Watson, G.N., 1927. A course of modern analysis. Cambridge.